Short communication

Dimethyl ether Carbonylation over Mordenite zeolite modified by Alkyimidazolium ions

Shiping Liu[a,1], Xudong Fang[a,b,a], Yong Liu[a], Hongchao Liu[a], Xiangang Ma[a], Wenliang Zhu[a], Zhongmin Liu[a,*]

[a] National Engineering Laboratory for Methanol to Olefins, Dalian National Laboratory for Clean Energy, Dalian Institute of Chemical Physics, Chinese Academy of Sciences, Dalian, 116023, China
[b] University of, Chinese Academy of Sciences, Chinese Academy of Sciences, Beijing 100049, China

ABSTRACT

Acidic mordenite zeolite was modified with various alkyimidazolium ions with different sizes via ion-exchange and applied as dimethyl ether (DME) carbonylation catalysts. Introducing 1, 3-dimethylimidazolium ions into zeolite can selectively remove the acid sites in 12-membered ring (MR) channels, significantly enhancing the stability and activity. Additionally, ion-exchange with organic ions was used to control the acid site distributions to separately investigate the DME carbonylation reaction in 8-MR and 12-MR channels. The reaction results indicated that the acid sites in 12-MR channels can concurrently catalyze the carbonylation and methanol-to-hydrocarbons (MTH) reactions, and MTH reactions seriously suppress the carbonylation activity in 8-MR channels.

1. Introduction

Dimethyl ether (DME) coupling with CO over acidic zeolites provides a non-noble metal catalysis and halide-free process to upgrade the widely available C1 intermediates into high value-added methyl acetate (MA), which can be facilely hydrogenated to ethanol [1–3]. Thus, the DME carbonylation is also considered as the key step for ethanol synthesis, which has attracted considerable attention in the past decade. Since Iglesia and co-workers [4–8] reported the selective DME carbonylation over acidic zeolites, various zeolites such as H-MOR [9], H−Y [4,10], H-ZSM-35 [11,12], H-ZSM-5 [13], H-EU-12 [14], and H-SSZ-13 [15] have been explored for the DME carbonylation reaction. Among these zeolites, H-MOR zeolite is the most active catalyst for DME carbonylation. The outstanding carbonylation activity is attributed to the special structural features of MOR zeolite, which contains two distinct types of cavities: 8-membered ring (8-MR) side pockets (4.8 × 3.4 Å) and 12-MR channels (6.5 × 7.0 Å). This large/small pores impose different constrains on the acid sites, leading to distinct catalytic behaviors in the reaction of DME carbonylation. Bhan et al.[6] and Shen et al. [16] found that the carbonylation activity was proportional to the number of acid sites in the small 8-MR channels, suggesting that the acidic sites in 8-MR channels were the active sites for carbonylation, which was confirmed by the theoretical studies from

Rasmussen and co-workers [17,18]. However, the acid sites in 12-MR channels are the active sites for the methanol-to-hydrocarbons (MTH) reactions and lead to deactivation because the 12-MR channels possess large void spaces to accommodate coke species, whereas coke formation is sterically inhibited in the small 8-MR channels [19]. As these two types of channels simultaneously function during the reaction, there is a possibility that the carbonylation and MTH reactions mutually influence each other. However, the interplay between them has been rarely investigated, which would restrict the comprehensive understanding of catalytic roles of acid sites in different channels. In order to clarify the relationship between carbonylation and MTH reactions, the DME carbonylation reaction in the 8-MR and 12-MR channels should be separately investigated, which requires the distribution of acid site in mordenite zeolite to be controlled.

Controlling the acid site distribution in mordenite zeolite is also helpful in solving the deactivation problem. As mentioned above, the acid sites in 12-MR channels result in deactivation. Therefore, it is feasible to prolong lifetime by eliminating the acid sites in 12-MR channels. For example, Liu et al. [20] demonstrated that pyridine could selectively poison the acid sites in 12-MR channels, remarkably improving the stability. However, Li et al. [21] suggested that coke intermediates formed in 12-MR channels would cause the desorption of

---

neighboring adsorbed pyridine, resulting in the acceleration of deactivation. In addition, literature reported that selective dealumination [22,23] and ion-exchange with metal ions [24–27] were effective to stabilize the H-MOR, but the reported lifetime hardly exceeded 100 h. Recently, we reported that tetramethylammonium cations (TMA$^+$) could selectively remove the acid sites in 12-MR channels, leading to an excellent stability for more than 210 h [28]. However, incorporating too many TMA$^+$ into 12-MR channels decreased the activity due to diffusion limitation. Inspired by that work, we employed alkyimidazolium ions to modify mordenite for DME carbonylation reaction. In addition, the acid site distributions in mordenite were controlled to investigate the catalytic roles of acid sites at 12-MR channels in DME carbonylation reaction.

2. Experimental

2.1. Catalysts preparation

Organic ions-modified catalysts were prepared by ion-exchange method. The H-type mordenite samples (H-MOR) were exchanged with different organic salts including 1-methylimidazole (mmiz) hydrochloride, 1, 3-dimethylimidazolium (dmim) chloride, and 1-butyl-3-methylimidazolium (bmim) chloride. The obtained samples were denoted as x-[mmiz]-MOR, x-[dmim]-MOR, and x-[bmim]-MOR, where x corresponds to the molar concentration of organic salts solution. The details of ion-exchange procedures were given in the Electronic Supplementary Information (ESI).

The 8Na-12H-MOR sample with acid sites solely in 12-MR channels was prepared using the previously reported protocol [28]. The Na-type mordenite sample was exchanged with tetramethylammonium chloride three times. The exchanged sample was then calcined at 550 °C for 4 h.

2.2. Catalysts characterization

The catalysts were characterized by multiple techniques including TG, FT-IR spectroscopy, N$_2$ adsorption-desorption, and intelligent gravimetric analyzer. The details of measurements were given in ESI.

2.3. Catalytic test

The DME carbonylation reaction condition used in this work was the same as that used in our previous work [28]. The details of catalytic reaction were provided in ESI.

3. Results and discussion

3.1. Catalyst characterization

3.1.1. Textural and structural properties

The structure parameters of H-MOR and organic ions-modified H-MOR samples are listed in Table 1. It can be seen that introducing organic ions into mordenite zeolite remarkably changes the textural properties of catalysts. Both the surface area and micropore volume sharply decrease. The surface area of 1.0-[bmim]-MOR sample even decreases to 62 m^2/g because the 12-MR channels are filled with the bulky [bmim]$^+$ ions. And it is found that the loadings of organic ions decrease with the increase of organic ion size. It is because that the ion-exchange behavior is closely associated with the organic ions size. The large ions are subjected to a higher diffusion resistance when travelling in the channels, which is unfavorable to ion-exchange. Meanwhile, the large ions suffer from steric restriction and have no access to the ion-exchange sites in small pores. As a result, the larger organic ions lead to lower adsorbed amounts.

The TG curves of organic ions-modified samples are given in Fig. S2. The mass losses below 250 °C are due to the vaporing of adsorbed water. At the high temperature stage, the mass losses are attributed to

Table 1
Textural properties of H-MOR and organic ions exchanged MOR samples.

Sample	Molar contents of organic ions (mmol/g) [a]	Specific surface area (m^2/g)[b]	Micropore volume (cm^3/g)[c]
H-MOR	–	532	0.16
1.0-[mmiz]-MOR	0.62	225	0.057
0.2-[dmim]-MOR	0.49	304	0.081
0.4-[dmim]-MOR	0.52	271	0.071
1.0-[dmim]-MOR	0.56	252	0.068
1.0-[bmim]-MOR	0.53	62	0.005

a: Weight loss in the temperature range of 250–700 °C, b: Calculated by Langmuir method, c: Calculated by t-plot method, the N$_2$ isotherms of all the exchanged samples are shown in Fig. S1.

the combustion of organic ions evidenced by the exothermic peaks at around 530 °C in the DSC curves. Such a high decomposition temperature suggests that the alkyimidazolium ions in zeolites are not prone to decomposition during the reaction. Comparing with the 1.0-[dmim]-MOR and 1.0-[mmiz]-MOR samples, the 1.0-[bmim]-MOR sample exhibits a lower decomposition temperature because of the [bmim]$^+$ ion with a long butyl group. Typically, longer alkyl groups make both the carbocation and carbon radicals more stable [29], thus the decomposition reaction occurs more easily.

3.1.2. FT-IR analysis

The IR spectra of H-MOR and organic ions-modified samples are presented in Fig. 1. With the H-MOR sample, the bands at 3747 and 3603 cm^{-1} attributed to the silanol groups and acidic OH groups, respectively, are observed. After exchanging with organic ions, the band at 3747 cm^{-1} is unaffected, but the intensity of acidic OH bands significantly decreases, suggesting that a portion of acid sites are removed. Moreover, it is found that the acidic OH bands shift from 3603 to 3583 cm^{-1}. It has been well accepted that the high frequency (~3610 cm^{-1}) and low frequency (~3585 cm^{-1}) bands correspond to the acid sites in 12-MR and 8-MR channels, respectively [30]. The shift of acidic OH bands toward low frequency suggests that the acid sites in 12-MR channels are selectively removed by organic ions. Unlike other organic ions, [mmiz]$^+$ ions lead to the complete disappearance of acidic OH bands, indicating that [mmiz]$^+$ ions have access to the acid sites in 8-MR channels. The IR spectra confirm that organic ions are incorporated into zeolites and have a great influence on the acid site distributions.

3.2. Catalytic studies

3.2.1. The catalytic roles of the acid sites in 12-MR channels

The distribution of acid site in 8Na-12H-MOR sample is investigated
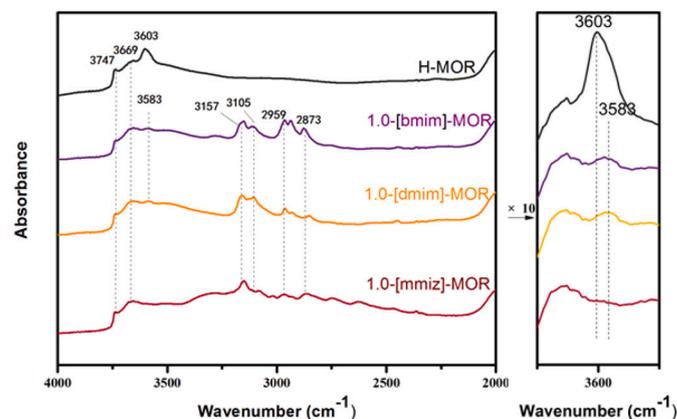
Fig. 1. FT-IR spectra of H-MOR and organic ions exchanged mordenite zeolites.
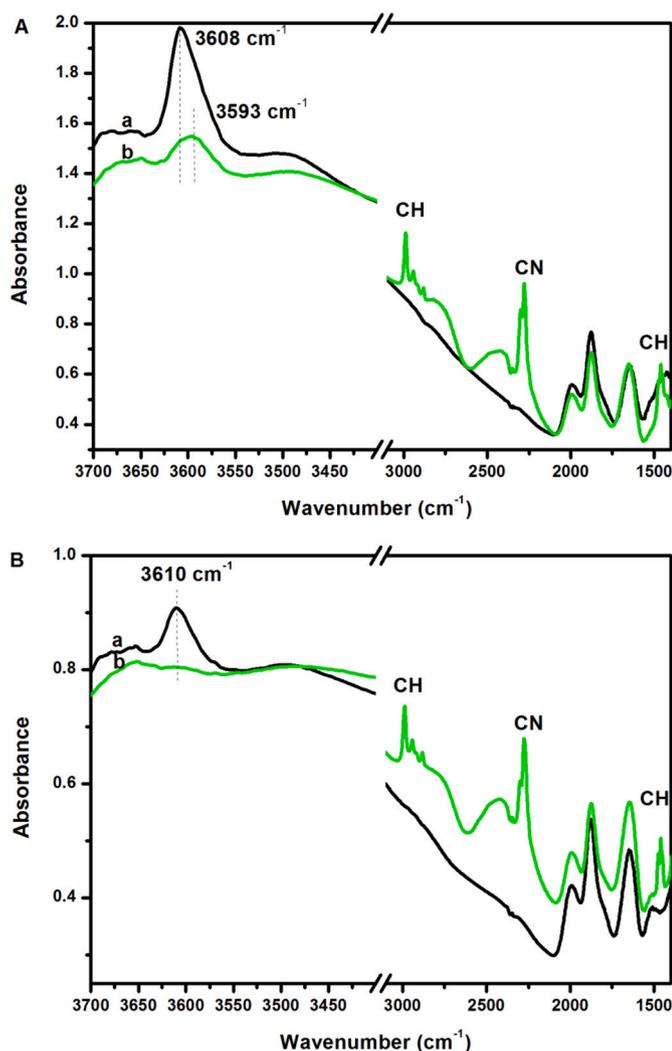
Fig. 2. FT-IR spectra of H-MOR (A) and 8Na-12H-MOR (B) before (a) and after (b) adsorbing IBN at 50 °C. All of the spectra were recorded at room temperature.

by FT-IR using isobutyronitrile (IBN) as the probe molecule (Fig. 2). The spectrum of the H-MOR sample after dehydration at 350 °C shows an asymmetrical band at 3608 cm^{-1}. After adsorbing IBN molecules, the intensity of acidic OH band significantly decreases, and a small peak at around 3593 cm^{-1} resists. As mentioned above, the high and low frequency bands should be attributed to the acid sites in 12-MR and 8-MR channels, respectively. This result confirms that both the 12-MR and 8-MR channels of H-MOR sample bear acid sites. With the 8Na-12H-MOR sample, the acidic OH stretching band at 3610 cm^{-1} can be observed, but this band completely disappears after contacting with IBN molecules, indicating that there are no protons in the 8-MR channels. Hence, according to the IR results, it can be concluded that the acid sites are solely located in the 12-MR channels of 8Na-12H-MOR sample. In addition, the sharp peaks of adsorbed IBN at 3000–2800 cm^{-1} (CH stretching), 2300–2230 cm^{-1} (CN stretching), and 1500–1200 cm^{-1} (CH deformation) are also observed.

As the distribution of acid site in mordenite zeolites can be controlled, the DME carbonylation reaction can be separately investigated in 8-MR and 12-MR channels. The reaction results of the samples with different acid site distributions are given in Fig. 3. After the induction period, the DME conversion of H-MOR sample reaches the maximum value of 32% and gradually decreases to 9% within 24 h. With the decrease of the carbonylation activity, the hydrocarbons selectivity increases as a result of the MTH reactions. Interestingly, the 8Na-12H-

MOR sample exhibits a DME conversion of 23%, suggesting that the acid sites in 12-MR channels contribute to the carbonylation activity. Though the previous literature proposed that the confinement effect plays a crucial role in the carbonylation reaction [5,10,31], these results demonstrate that carbonylation also occurs within less confining voids. For the H-MOR sample, both 8-MR and 12-MR channels have contribution to the DME conversion. According to the difference in the DME conversion between H-MOR and 8Na-12H-MOR samples, it can be estimated that only 9% of DME conversion is contributed by the acid sites in 8-MR channels of H-MOR sample. In our previous work [28], the ion-exchange studies have demonstrated that the acid sites in 8-MR channels account for 32% of the total acid sites. Thus, it seems that the carbonylation activity of the acid sites in 8-MR channels is not higher than that of the acid sites in 12-MR channels, which is contrary to the opinion that the carbonylation reaction mainly takes place in the 8-MR channels. However, after modifying with [dmim]$^+$ ions, the carbonylation activity significantly increases and increases with increasing the amounts of [dmim]$^+$ ions. The number of acid sites decreases with increasing the concentration of [dmim]$^+$ ions, but the DME conversion increases, indicating that the [dmim]$^+$ ions have a promotional effect on the carbonylation. Typically, metal ions were found to promote the carbonylation since metal ions can activate CO. [27] As for the [dmim]$^+$ ions, they are located at 12-MR channels while the carbonylation mainly occurs in 8-MR channels. It is impossible for [dmim]$^+$ ions to promote the carbonylation in the manner of metal ions. We speculate that the higher carbonylaion activity of the [dmim]$^+$ ions-modified catalysts is caused by the suppression of MTH reactions in 12-MR channels, because MTH reactions also produce water that can inhibit the carbonylation reaction.[4, 6, 28]The selective removal of acid sites in 12-MR channels by [dmim]$^+$ ions can supress MTH reactions, thereby promoting the carbonylation. In order to confirm this assumption, we compare the catalytic performance of H-MOR and 1.0-[dmim]-MOR at 150 °C (Fig.S3). As MTH reactions are severely supressed at low temperature, the supressing effect of MTH reactions on the carbonylation is not obvious over H-MOR. These two catalysts present similar catalytic performance, demonstrating that the promotional effect of [dmim]$^+$ ions is associated with MTH reactions. Suppressing MTH reactions by the [dmim]$^+$ ions can be evidenced by the enhanced stability. No obvious deactivation is observed over the [dmim]$^+$ ions-modified catalysts within 24 h.

3.3. 3.2. 2. The effect of alkyimidazolium ions on the catalytic performance

Furthermore, a series of alkyimidazolium ions are employed to investigate the effect of the organic ions size on the catalytic performance (Fig. 4). Interestingly, all the samples display excellent stability in DME carbonylation reaction. After at least 62 h on stream, no sight of deactivation is observed, suggesting that the alkyimidazolium ions-modified catalysts are resistant to coke formation. The excellent stability is attributed to the unique geometry of the alkyimidazolium ions. The alkyimidazolium ions have a flat geometry, whereas the highly branched alkylammonium ions are nearly spherical. Generally, the plate-like alkyimidazolium ions occupy less pore space than the spherical alkylammonium ions. For example, the 1.0-[dmim]-MOR sample shows larger micropore volume than the TMA-exchanged sample used in the previous work [28], although the amount of [dmim]$^+$ ions is the same as that of TMA$^+$ ions (0.56 mmol/g). Larger pore volume means that there is more accessible pore space for the mass transfer. Hence, coke precursor species formed in the micropores can diffuse out more easily, making 1.0-[dmim]-MOR catalyst less susceptible to deactivation. Additionally, it is found that there is a great difference in the activity between the alkyimidazolium ions exchanged catalysts. The small [mmiz]$^+$ ions lead to a DME conversion of 4%. The low activity is full agreement with the absence of acidic sites in 8-MR channels, which is evidenced by the IR spectra shown in Fig. 1. The diameter of [mmiz]$^+$ ion is about 4.5 Å [32], which is slightly smaller than the opening of 8-
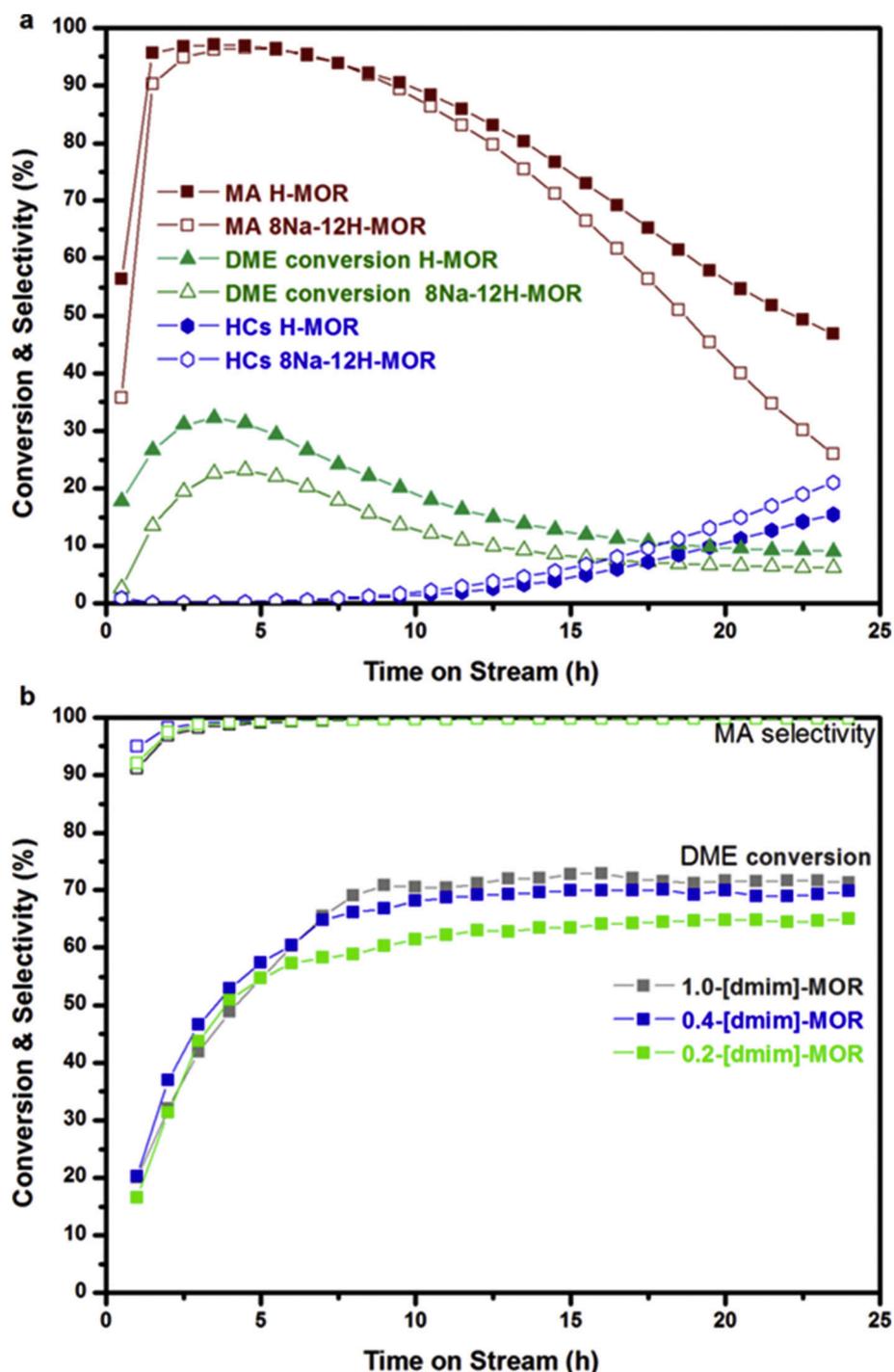
Fig. 3. The catalytic performance of (a) H-MOR and 8Na-12H-MOR, (b) [dmim] ions exchanged MOR samples. Reaction condition: DME/CO/N_2 = 5/35/60, 200 °C, 2.0 MPa, GHSV = 2250 mL/g_{cat}·h.

MR side pockets. The [mmiz]$^+$ ions can enter the 8-MR channels and cover the acid sites, resulting in the lowest carbonylation activity among the three samples. Compared with the [mmiz]$^+$ ion, the [dmim]$^+$ ion has a more methyl group, which is larger than the [mmiz]$^+$ ion. The steric hindrance would make the [dmim]$^+$ ions inaccessible to the acid sites in 8-MR channels. Consequently, the DME conversion significantly increases to 70%. Moreover, the 1.0-[dmim]-MOR catalyst also exhibits good stability. This result demonstrates that excellent stability and high activity could be concomitantly achieved over 1.0-[dmim]-MOR catalyst, making it attractive for industrial application. When using the large [bmim]$^+$ ions, although the acid sites in

8-MR channels are not affected, the 1.0-[bmim]-MOR catalyst presents a low DME conversion, only 25%. Differing from the [dmim]$^+$ ion, the [bmim]$^+$ ion has a large butyl group. Incorporating the bulky [bmim]$^+$ ions into 12-MR channels would lead to pore-blockage, thus affecting the diffusion of reactants and products molecules in 12-MR channels. This can be confirmed by the MA adsorption experiments. As shown in Fig. S4a, the 1.0-[bmim]-MOR sample shows lower MA adsorption capacity compared with 1.0-[dmim]-MOR. Moreover, it can be seen that the MA uptake rate of 1.0-[bmim]-MOR sample is lower than that of 1.0-[dmim]-MOR during the initial 200 s (Fig. S4b), giving clear evidence that large [bmim]$^+$ ions can lead to the diffusion limitation. As a
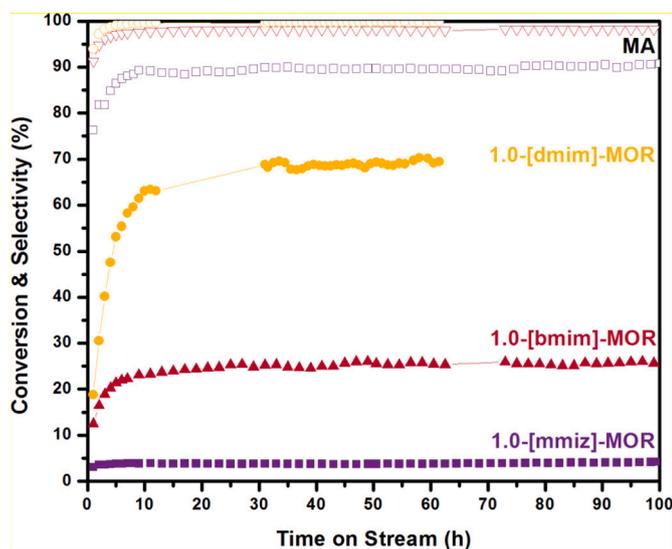
Fig. 4. The catalytic performance of alkyimidazolium ions exchanged MOR samples; open symbols: methyl acetate selectivity, solid symbols: DME conversions. Reaction condition: DME/CO/N$_2$ = 5/35/60, 200 °C, 2.0 MPa, GHSV = 2250 mL/g$_{cat}$·h.

result, a low activity is achieved over 1.0-[bmim]-MOR.

4. Conclusion

In summary, the DME carbonylation reaction in different channels of mordenite zeolites reveals that the acid sites in 12-MR channels concurrently catalyze the MTH and carbonylation reactions, and the MTH reactions in 12-MR channels not only lead to deactivation but also depress the carbonylation in 8-MR channels. In addition, the reaction results of organic ions-modified mordenite catalysts demonstrate that the size of organic ions is the key factor governing the catalytic performance. By choosing the proper ions with the appropriate size, for example, [dmim]$^+$ ion, both excellent stability and high activity can be achieved over the alkyimidazolium ions-modified catalysts. The present work would deepen the understanding of the roles of acid sites at 12-MR channels in DME carbonylation reaction and presents an effective approach to improve the catalytic performance.

Declaration of Competing Interest

None.

Acknowledgements

Credit Author Statement.

Shiping Liu: **Conceptualization**, **Investigation**,**Writing-Original Draft**.

Xudong Fang: **Investigation**, **Writing-Original Draft**.

Yong Liu: **Investigation**, **Visualization**.

Hongchao Liu: **Resources**, **Investigation**.

Xiangang Ma: **Investigation**, **Validation**.

Jindou Huang **Investigation**, **Resources**.

Wenliang Zhu and Zhongmin Liu: **Conceptualization**, **Supervision**, **Writing - Review & Editing**.

Declaration of interests

☒ The authors declare that they have no known competing financial interests or personal relationships that could have appeared to influence the work reported in this paper.

Appendix A. Supplementary data

Supplementary material.

References

[1] X. Li, X. San, Y. Zhang, T. Ichii, M. Meng, Y. Tan, N. Tsubaki, Direct synthesis of ethanol from dimethyl ether and syngas over combined H-Mordenite and cu/ZnO catalysts, ChemSusChem 3 (2010) 1192–1199.

[2] P. Lu, G.H. Yang, Y. Tanaka, N. Tsubaki, Ethanol direct synthesis from dimethyl ether and syngas on the combination of noble metal impregnated zeolite with cu/ZnO catalyst, Catal. Today 232 (2014) 22–26.

[3] X.G. San, Y. Zhang, W.J. Shen, N. Tsubaki, New synthesis method of ethanol from dimethyl ether with a synergic effect between the zeolite catalyst and metallic catalyst, Energy Fuel 23 (2009) 2843–2844.

[4] P. Cheung, A. Bhan, G.J. Sunley, E. Iglesia, Selective Carbonylation of dimethyl ether to methyl acetate catalyzed by acidic zeolites, Angew. Chem. Int. Ed. 45 (2006) 1617–1620.

[5] A. Bhan, A.D. Allian, G.J. Sunley, D.J. Law, E. Iglesia, Specificity of sites within eight-membered ring zeolite channels for carbonylation of methyls to acetyls, J. Am. Chem. Soc. 129 (2007) 4919–4924.

[6] P. Cheung, A. Bhan, G. Sunley, D. Law, E. Iglesia, Site requirements and elementary steps in dimethyl ether carbonylation catalyzed by acidic zeolites, J. Catal. 245 (2007) 110–123.

[7] A. Bhan, E. Iglesia, A link between reactivity and local structure in acid catalysis on zeolites, Acc. Chem. Res. 41 (2008) 559–567.

[8] E.S. Zhan, Z.P. Xiong, W.J. Shen, Dimethyl ether carbonylation over zeolites, J. Energy. Chem. 36 (2019) 51–63.

[9] N. Zhao, Q.P. Cheng, S.S. Lyu, L.H. Guo, Y. Tian, T. Ding, J. Xu, X.B. Ma, X.G. Li, Promoting dimethyl ether carbonylation over hot-water pretreated H-mordenite, Catal. Today 339 (2020) 86–92.

[10] M. Boronat, C. Martinez-Sanchez, D. Law, A. Corma, Enzyme-like specificity in zeolites: a unique site position in Mordenite for selective Carbonylation of methanol and dimethyl ether with CO, J. Am. Chem. Soc. 130 (2008) 16316–16323.

[11] X. Li, X. Liu, S. Liu, S. Xie, X. Zhu, F. Chen, L. Xu, Activity enhancement of ZSM-35 in dimethyl ether carbonylation reaction through alkaline modifications, RSC Adv. 3 (2013) 16549–16557.

[12] J. Liu, H. Xue, X. Huang, Y. Li, W. Shen, Dimethyl ether Carbonylation to methyl acetate over HZSM-35, Catal. Lett. 139 (2010) 33–37.

[13] S. Wang, S.Y. Li, L. Zhang, Z.F. Qin, Y.Y. Chen, M. Dong, J.F. Li, W.B. Fan, J.G. Wang, Mechanistic insights into the catalytic role of various acid sites on ZSM-5 zeolite in the carbonylation of methanol and dimethyl ether, Catal. Sci. Technol. 8 (2018) 3193–3204.

[14] X.B. Feng, J. Yao, H.J. Li, Y. Fang, Y. Yoneyama, G.H. Yang, N. Tsubaki, A brand new zeolite catalyst for carbonylation reaction, Chem. Commun. 55 (2019) 1048–1051.

[15] M. Lusardi, T.T. Chen, M. Kale, J.H. Kang, M. Neurock, M.E. Davis, Carbonylation of dimethyl ether to methyl acetate over SSZ-13, ACS Catal. 10 (2020) 842–851.

[16] H.B. Sheng, W.X. Qian, H.T. Zhang, P. Zhao, H.F. Ma, W.Y. Ying, Synthesis of hierarchical porous H-mordenite zeolite for carbonylation of dimethyl ether, Micro. Meso. Mater., 295 (2020).

[17] D.B. Rasmussen, J.M. Christensen, B. Temel, F. Studt, P.G. Moses, J. Rossmeisl, A. Riisager, A.D. Jensen, Ketene as a reaction intermediate in the Carbonylation of dimethyl ether to methyl acetate over Mordenite, Angew. Chem. Int. Ed. 54 (2015) 7261–7264.

[18] D.B. Rasmussen, J.M. Christensen, B. Temel, F. Studt, P.G. Moses, J. Rossmeisl, A. Riisager, A.D. Jensen, Reaction mechanism of dimethyl ether carbonylation to methyl acetate over mordenite a combined DFT/experimental study, Catal. Sci. Technol. 7 (2017) 1141–1152.

[19] M. Boronat, C. Martínez, A. Corma, Mechanistic differences between methanol and dimethyl ether carbonylation in side pockets and large channels of mordenite, Phys. Chem. Chem. Phys. 13 (2011) 2603.

[20] J. Liu, H. Xue, X. Huang, P. Wu, S. Huang, S. Liu, W. Shen, Stability enhancement of H-Mordenite in dimethyl ether Carbonylation to methyl acetate by pre-adsorption of pyridine, Chin. J. Catal. 31 (2010) 729–738.

[21] Y. Li, Q. Sun, S.Y. Huang, Z.Z. Cheng, K. Cai, J. Lv, X.B. Ma, Dimethyl ether carbonylation over pyridine-modified MOR: enhanced stability influenced by acidity, Catal. Today 311 (2018) 81–88.

[22] H.F. Xue, X.M. Huang, E.S. Zhan, M. Ma, W.J. Shen, Selective dealumination of mordenite for enhancing its stability in dimethyl ether carbonylation, Catal. Commun. 37 (2013) 75–79.

[23] X.S. Wang, R.J. Li, C.C. Yu, Y.X. Liu, L.Y. Zhang, C.M. Xu, H.J. Zhou, Enhancing the dimethyl ether carbonylation performance over mordenite catalysts by simple alkaline treatment, Fuel 239 (2019) 794–803.

[24] T. Blasco, M. Boronat, P. Concepción, A. Corma, D. Law, J.A. Vidal-Moya, Carbonylation of methanol on metal–acid zeolites: evidence for a mechanism

involving a multisite active center, Angew. Chem. Int. Ed. 119 (2007) 4012–4015.

[25] M. Ma, E.S. Zhan, X.M. Huang, N. Ta, Z.P. Xiong, L.Y. Bai, W.J. Shen, Carbonylation of dimethyl ether over co-HMOR, Catal. Sci. Technol. 8 (2018) 2124–2130.

[26] A.A.C. Reule, N. Semagina, Zinc hinders deactivation of copper-Mordenite: dimethyl ether Carbonylation, ACS Catal. 6 (2016) 4972–4975.

[27] T. Blasco, M. Boronat, P. Concepción, A. Corma, D. Law, J.A. Vidal-Moya, Carbonylation of methanol on metal–acid zeolites: evidence for a mechanism involving a multisite active center, Angew. Chem. Int. Ed. 46 (2007) 3938–3941.

[28] S.P. Liu, H.C. Liu, X.G. Ma, Y. Liu, W.L. Zhu, Z.M. Liu, Identifying and controlling the acid site distributions in mordenite zeolite for dimethyl ether carbonylation reaction by means of selective ion-exchange, Catal. Sci. Technol. 10 (2020)

4663–4672.

[29] Y.Y. Cao, T.C. Mu, Comprehensive investigation on the thermal stability of 66 ionic liquids by thermogravimetric analysis, Ind. Eng. Chem. Res. 53 (2014) 8651–8664.

[30] V.L. Zholobenko, M.A. Makarova, J. Dwyer, Inhomogeneity of Broensted acid sites in H-mordenite, J. Phys. Chem. 97 (1993) 5962–5964.

[31] Y.Y. Chu, A.Y. Lo, C. Wang, F. Deng, Origin of high selectivity of dimethyl ether Carbonylation in the 8-membered Ring Channel of Mordenite zeolite, J. Phys. Chem. C 123 (2019) 15503–15512.

[32] J.A. Harvey, S.M. Auerbach, Simulating hydrogen-bond structure and dynamics in glassy solids composed of imidazole oligomers, J. Phys. Chem. B 118 (2014) 7609–7617.